JGP Journal of General Physiology

COMMUNICATION

Regulation of heart rate and the pacemaker current by phosphoinositide 3-kinase signaling

Richard Z. Lin[1,2*], Zhongju Lu[1,4*], Evgeny P. Anyukhovsky[1], Ya-Ping Jiang[1], Hong Zhan Wang[1], Junyuan Gao[1], Michael R. Rosen[1,3], Lisa M. Ballou[1], and Ira S. Cohen[1]

Heart rate in physiological conditions is set by the sinoatrial node (SN), the primary cardiac pacing tissue. Phosphoinositide 3-kinase (PI3K) signaling is a major regulatory pathway in all normal cells, and its dysregulation is prominent in diabetes, cancer, and heart failure. Here, we show that inhibition of PI3K slows the pacing rate of the SN in situ and in vitro and reduces the early slope of diastolic depolarization. Furthermore, inhibition of PI3K causes a negative shift in the voltage dependence of activation of the pacemaker current, I_F, while addition of its second messenger, phosphatidylinositol 3,4,5-trisphosphate, induces a positive shift. These shifts in the activation of I_F are independent of, and larger than, those induced by the autonomic nervous system. These results suggest that PI3K is an important regulator of heart rate, and perturbations in this signaling pathway may contribute to the development of arrhythmias.

Introduction

The heartbeat normally originates in myocytes of the sinoatrial node (SN), the primary cardiac pacemaker. Evidence exists for both voltage-dependent and calcium-dependent "clocks" that determine the spontaneous rhythmicity of the SN (Eisner and Cerbai, 2009). A major component of the voltage-dependent mechanism is the hyperpolarization-activated pacemaker current, I_F. The autonomic nervous system modulates both heart rate and I_F (DiFrancesco, 2006). Here we show that phosphoinositide 3-kinase (PI3K), an enzyme whose dysregulation underlies a number of pathological conditions including diabetes, long QT syndrome (a pathological increase in the interval between the Q and T waves on the electrocardiogram), and cancer, alters the endogenous rate of the SN and I_F independently of the autonomic nervous system. These findings are relevant to those disease states, as an increase in sympathetic tone required to compensate for the slowing induced by PI3K inhibition is itself arrhythmogenic.

Materials and methods

Experimental animals

All animal-related procedures were approved by the Stony Brook University Institutional Animal Care and Use Committee. Male C57BL/6J mice were purchased from The Jackson Laboratory and were studied at 2–3 mo of age. New Zealand White rabbits (1.3–1.8 kg) were purchased from Charles River Laboratories. Adult male mongrel dogs (20–28 kg) were purchased from Covance Laboratories.

Recording of mouse cardiac electrical activity ex vivo

Isolated hearts were mounted on the IH-SR isolated heart perfusion system (Harvard Apparatus) and perfused with Krebs-Henseleit solution (118 mM NaCl, 4.7 mM KCl, 2.52 mM $CaCl_2$, 1.64 mM $MgSO_4$, 24.88 mM $NaHCO_3$, 1.18 mM KH_2PO_4, 5.55 mM glucose, and 2 mM sodium pyruvate, aerated with 5% CO_2 and 95% O_2) at 37°C. For electrocardiographic recording, one electrode was placed at the base of the heart next to the left atrium, and a second electrode was placed at the heart apex. Data were collected using the LabChart Pro 8.1.5 (ADInstruments) software system. When the heart rate reached a stable baseline, vehicle (dimethylsulfoxide) or PI-103 (Cayman Chemical) was added to the perfusate reservoir and circulated through the heart for 30 min before collecting the first set of data. Then isoproterenol (Iso; Sigma-Aldrich) was added to the perfusate reservoir and circulated through the heart for another 30 min before collecting the second set of data. The number of heartbeats in a 10-s portion of the recording was counted, and heart rate in beats per minute (bpm) was calculated.

[1]Department of Physiology and Biophysics, Stony Brook University, Stony Brook, NY; [2]Medical Service, Northport VA Medical Center, Northport, NY; [3]Departments of Pharmacology and Pediatrics, Columbia University, New York, NY; [4]Department of Medicine, Stony Brook University, Stony Brook, NY.

*R.Z. Lin and Z. Lu contributed equally to this paper; Correspondence to Ira S. Cohen: Ira.Cohen@stonybrook.edu.

Recording of canine SN electrical activity ex vivo

Dogs were anesthetized with propofol (6–8 mg/kg intravenous) followed by inhalational isoflurane 2.5–3.5% and oxygen. Hearts were rapidly removed through a left thoracotomy and immersed in cold Tyrode's solution (131 mM NaCl, 18 mM $NaHCO_3$, 1.8 mM $CaCl_2$, 0.5 mM $MgCl_2$, 1.8 mM NaH_2PO_4, and 5.5 mM dextrose, aerated with 5% CO_2 and 95% O_2). For experiments with isolated SN preparations, the solution also contained 4.0 mM KCl. Recently we described an isolated superfused canine SN preparation that maintains a stable beating rate and maximum diastolic potential (MDP) for several hours (Sosunov and Anyukhovsky, 2012). Similar SN preparations were used in the present study. The preparations were placed in a tissue bath, superfused with Tyrode's solution (37°C, pH 7.3–7.4), and allowed to beat spontaneously. Conventional microelectrode techniques were used to record transmembrane potentials. After 1 h in control Tyrode's solution, baseline recordings were made. The preparations were then superfused for 180 min with either control solution or solution containing 1 µM PI-103. Then 0.1 µM Iso was added for 5 min. The last records were made 15 min after Iso washout.

Measurement of I_F by patch clamp

Single SN myocytes were isolated from rabbit hearts as previously described (Tromba and Cohen, 1990). Electrophysiological measurements of I_F were performed in isolated rabbit SN cells at room temperature (20°C ± 1°C). The external solution contained 140 mM NaCl, 8 mM KCl, 1.8 mM $CaCl_2$, 1.0 mM $MgCl_2$, 5 mM HEPES, 10.0 mM glucose, 2 mM $MnCl_2$, 0.2 mM $CdCl_2$, and 8 mM $BaCl_2$ (pH adjusted to 7.4 with NaOH). The internal solution contained 50 mM KCl, 80 mM K-aspartate, 1 mM $MgCl_2$, 10 mM EGTA, 3 mM Mg-ATP, and 10 mM HEPES (pH 7.2). Mn^{2+} and Cd^{2+} were used to reduce Ca^{2+} currents, which can overlap with and obscure I_F tail currents. Ba^{2+} was used to block the background K^+ current (I_{K1}), which activates and inactivates in the same voltage range as I_F. The liquid junction potential (10 mV) between the electrode tip and cell interior was not corrected. Currents were measured in whole-cell patch-clamp mode using an Axopatch-1D amplifier. The pipettes had a resistance of 3 to 5 MΩ. The data were acquired and analyzed with pClamp software (version 9, Axon U.S.A.). Phosphoinositides (Echelon Biosciences) including the PI3K second messenger, phosphatidylinositol 3,4,5-trisphosphate ($PI(3,4,5)P_3$), were diluted in internal solution to a final concentration of 1 µM and infused through the patch pipette. Where indicated, cells were pretreated in bath solution with PI-103 for 2 h at room temperature before patch clamping. Carbachol (CCh; Sigma-Aldrich) and Iso were freshly prepared in distilled water before the experiment.

The voltage-clamp protocol for I_F activation was to apply 1-s hyperpolarizing voltage steps ranging from −30 mV to −110 mV in −10-mV increments from a holding potential of −30 mV and then to apply a depolarizing step to +50 mV for 0.5 s to record the tail currents, after which the preparation was stepped back to the holding potential. In some experiments, steps to −120 mV or −130 mV were achieved. In another protocol to measure peak magnitude and the time constant of activation, I_F was elicited by applying a 1.5-s hyperpolarizing pulse at −110 mV from a holding potential of −30 mV. The isochronal (IC) activation curves of I_F were fitted to the Boltzmann equation $gf(V) = gf,max * y\infty(V) = gf,max * \{1 + \exp[(V - V_{1/2})/K]\}$, where $V_{1/2}$ is the half-maximal voltage and K is the slope factor. When comparing different sets of data, statistical analysis was performed with either Student's t tests or ANOVA; significance was set to $P \leq 0.05$. Results are given as mean ± SEM.

Steady-state (SS) estimates of current magnitude and activation curves were generated by fitting the IC data to SS assuming that the relaxation was exponential after the initial delay. The start of the fit was roughly 20 ms after the initiation of the voltage step to roughly 10 ms before its end (there were slight variations based on the experimental data). Fig. S1 shows the raw data for one experiment in black with the exponential fits in red, demonstrating the assumption of a single exponential decay is justified. The SS currents were generated from −80 mV or −90 mV to the most negative potentials for which experimental data were available. The tail currents were then multiplied by the ratio of the SS amplitude at a given voltage to the IC amplitude to generate the theoretical SS tails, which were then fit to the Boltzman equation as described for the IC activation curves. Since the SS activation curves were all within a few percent of unity at −110 mV, the SS calculation for that experimental data at that voltage was used to estimate the maximal I_F density for comparison between experimental conditions.

Online supplemental material

Fig. S1 shows experimental IC current traces of I_F activation overlaid with estimates generated by fitting the IC data to SS. The traces are indistinguishable. Fig. S2 shows I_F activation curves generated by fitting IC data to SS. $V_{1/2}$ is shifted to more negative potentials in cells treated with PI-103. This shift is reversed by infusion of $PI(3,4,5)P_3$ through the patch pipette. Fig. S3 shows I_F activation curves generated by fitting IC data to SS. $V_{1/2}$ is shifted to more positive potentials in cells infused with $PI(3,4,5)P_3$ through the patch pipette. Fig. S4 shows I_F activation curves generated by fitting IC data to SS. $V_{1/2}$ in cells incubated with PI-103 is shifted to more positive potentials after treatment with Iso. Table S1 shows SS estimates of I_F current density at −110 mV. Exposure of rabbit SN myocytes to PI-103, Iso, or $PI(3,4,5)P_3$ did not significantly alter current density.

Results

In a previous study on drug-induced long QT syndrome, we noticed that pharmacologic and genetic down-regulation of PI3K signaling appeared to reduce the spontaneous beating rate of isolated, perfused mouse hearts (Lu et al., 2012). To further investigate this observation, we mounted mouse hearts on a Langendorff apparatus, perfused them with or without a pan-isoform PI3K inhibitor (PI-103), and determined heart rate from recordings of cardiac electrical activity. Control mouse hearts perfused with vehicle had a spontaneous rate of 418 ± 17 bpm that increased to 559 ± 15 bpm after exposure to Iso (Fig. 1). Mouse hearts treated with PI-103 beat at only 90% of the rate of control hearts (377 ± 26 bpm) but still manifested a strong response to Iso stimulation (524 ± 23 bpm; Fig. 1). We also

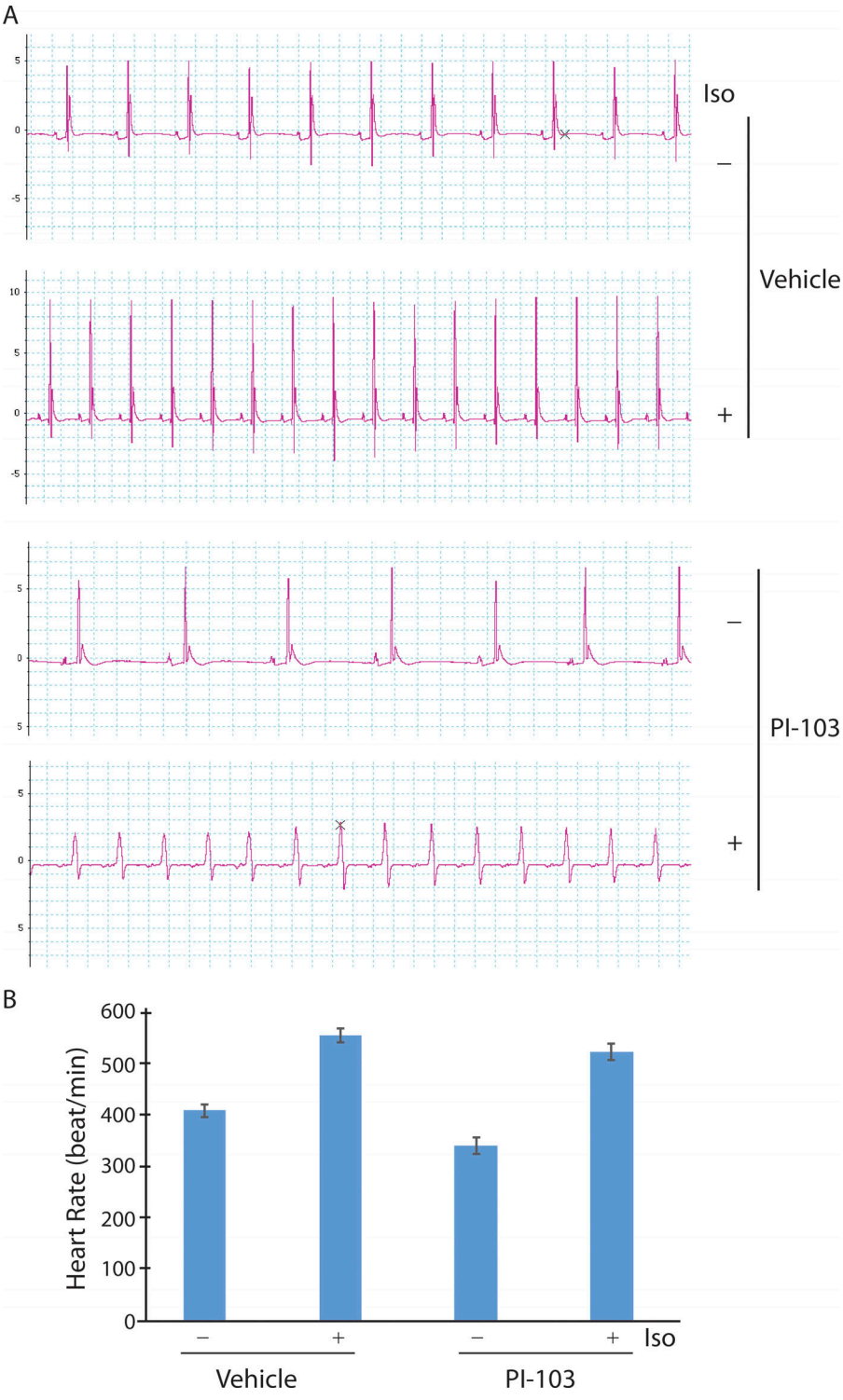

Figure 1. **Effects of PI-103 and Iso on mouse heart rate ex vivo. (A)** Representative tracings of cardiac electrical activity recorded from spontaneously beating hearts mounted on a Langendorff apparatus. Hearts were treated for 30 min with vehicle or 1 µM PI-103 (n = 3 per group) added to the perfusate, then for 30 min with or without 10 µM Iso. **(B)** Summary graph of heart rate shows mean ± SEM. Vehicle – Iso versus + Iso, P = 0.001; PI-103 – Iso versus + Iso and vehicle – Iso versus PI-103 – Iso, P = 0.03; vehicle + Iso versus PI-103 + Iso, P = 0.20; Student's t test.

calculated mean heart rate from recordings of perfused wild-type (n = 8) and PI3K p110α knockout (n = 4) hearts (Lu et al., 2012) and found that PI3K ablation caused a 9% decrease in rate (418 ± 7 bpm [wild type] versus 380 ± 18 bpm [knockout]; P < 0.05; t test). These results suggest that PI3K signaling modulates heart rate independently of sympathetic control.

The mouse heart beats much more rapidly than the human heart, so we next investigated the effects of PI3K inhibition on the cardiac rate of the adult dog, whose heart rate is closer to that of the human. We used ex vivo preparations of the SN in order to study heart rate independently of the autonomic nervous system. The left panel of Fig. 2 A shows a tracing of transmembrane potentials from a control SN that had stabilized to a constant rate after equilibrating for 1 h in the bath, and the adjacent panel shows the same control preparation 180 min later. There was no difference in rate. Rate increased from 108

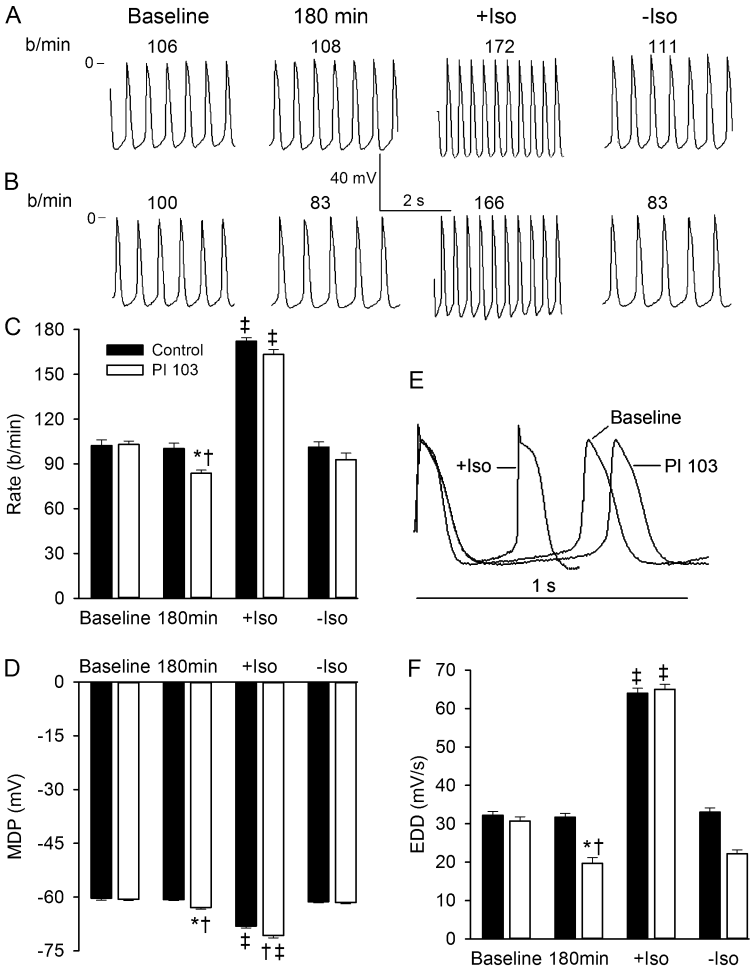

Figure 2. **Effects of PI-103 and Iso on canine SN automaticity. (A and B)** Representative transmembrane potentials recorded from spontaneously beating SN preparations. After baseline recording in control Tyrode's solution, tissue was superfused for 180 min with (A) control Tyrode's solution or (B) Tyrode's solution containing 1 µM PI-103. Then 0.1 µM Iso was added for 5 min (+Iso). The last records were made 15 min after Iso washout (-Iso). The numbers at the top of each record show the rate in beats per minute (b/min). **(C and D)** Summary data showing effects of PI-103 and Iso on rate and MDP, respectively. **(E)** Action potential traces from (B) recorded at baseline, following superfusion with PI-103, and after addition of Iso are superimposed, and shown with an expanded time scale. To better compare the slopes of diastolic depolarization, MDP of all traces is set at the same level. **(F)** Summary data for EDD. *, $P < 0.05$ versus PI-103 baseline; †, $P < 0.05$ versus 180 min control; ‡, $P < 0.05$ versus respective baseline, 180 min, and -Iso ($n = 6$ per group). Summarized data show mean ± SEM.

bpm to 172 bpm in response to 5 min of superfusion with Iso, as shown in the third panel. Rate returned to the control range after a 15-min washout of the sympathetic agonist, as shown in the right panel of Fig. 2 A. Fig. 2 B shows data for a similar experiment in which the preparation was superfused with PI-103 after equilibrating to a constant rate at baseline. The rate declined from 100 bpm to 83 bpm after 180 min in the presence of the PI3K inhibitor. Exposure to Iso increased the rate to 166 bpm, and again this increase was completely reversed upon washout (right panel). Fig. 2 C plots the average rate in all of the experimental conditions above for the six preparations studied in each group. There was a significant decrease in pacing rate after the 180-min incubation with PI-103 as compared with control. Both control and PI-103–treated preparations responded well to Iso, although there was a trend for the rate to be lower in preparations superfused with PI-103. Fig. 2 D shows that the MDP was significantly more negative in the PI-103–treated preparations. Iso also caused a significant hyperpolarization of the MDP for both control and PI-103 conditions. This was reversed upon washout (Fig. 2 D). To better visualize the slope of early diastolic depolarization (EDD), representative action potentials from Fig. 2 B were replotted vertically on an expanded time scale so that the MDPs appear identical (Fig. 2 E). The EDD slope at baseline was larger than that after 180 min with PI-103, consistent with the higher spontaneous rate at baseline. An action potential in the presence of Iso is also plotted to demonstrate the expected increase in EDD that led to the Iso-induced increase in beating rate (Fig. 2 E). Averaged values for EDD slope for all conditions show a significant reduction in the presence of PI-103 and a doubling in the presence of Iso that was reversed upon washout (Fig. 2 F). These results demonstrate that inhibition of PI3K leads to a reduction in beating rate in canine SN preparations without altering the robust effect of Iso.

We used myocytes isolated from the rabbit SN to study the effects of PI-103 on I_F because they are considered to be the most robust model to study this current (DiFrancesco et al., 1986). Rabbit SN myocytes were incubated for 2 h in the absence or presence of PI-103, and I_F was activated for 1 s by the voltage protocol shown in Fig. 3 A. The tail currents were then used to construct IC activation curves from which $V_{1/2}$ was calculated (Fig. 3 B). The results indicate that PI-103 treatment caused a negative shift of 15.9 mV in $V_{1/2}$ (−77.3 ± 0.7 mV [control] versus −93.2 ± 1.2 mV [PI-103]). If the shift in voltage dependence is due to inhibition of PI3K, this effect should be reversed by infusion of the PI3K second messenger, PI(3,4,5)P_3, through the patch pipette. Indeed, PI(3,4,5)P_3 infusion of cells incubated for 2 h with PI-103 resulted in an 11.7-mV positive shift in the midpoint voltage of the IC activation curve as compared with PI-103 treatment alone ($V_{1/2}$ = −81.0 ± 0.9 mV [PI-103 + PI(3,4,5)P_3]; Fig. 3 B). Shifts in voltage dependence should be accompanied by

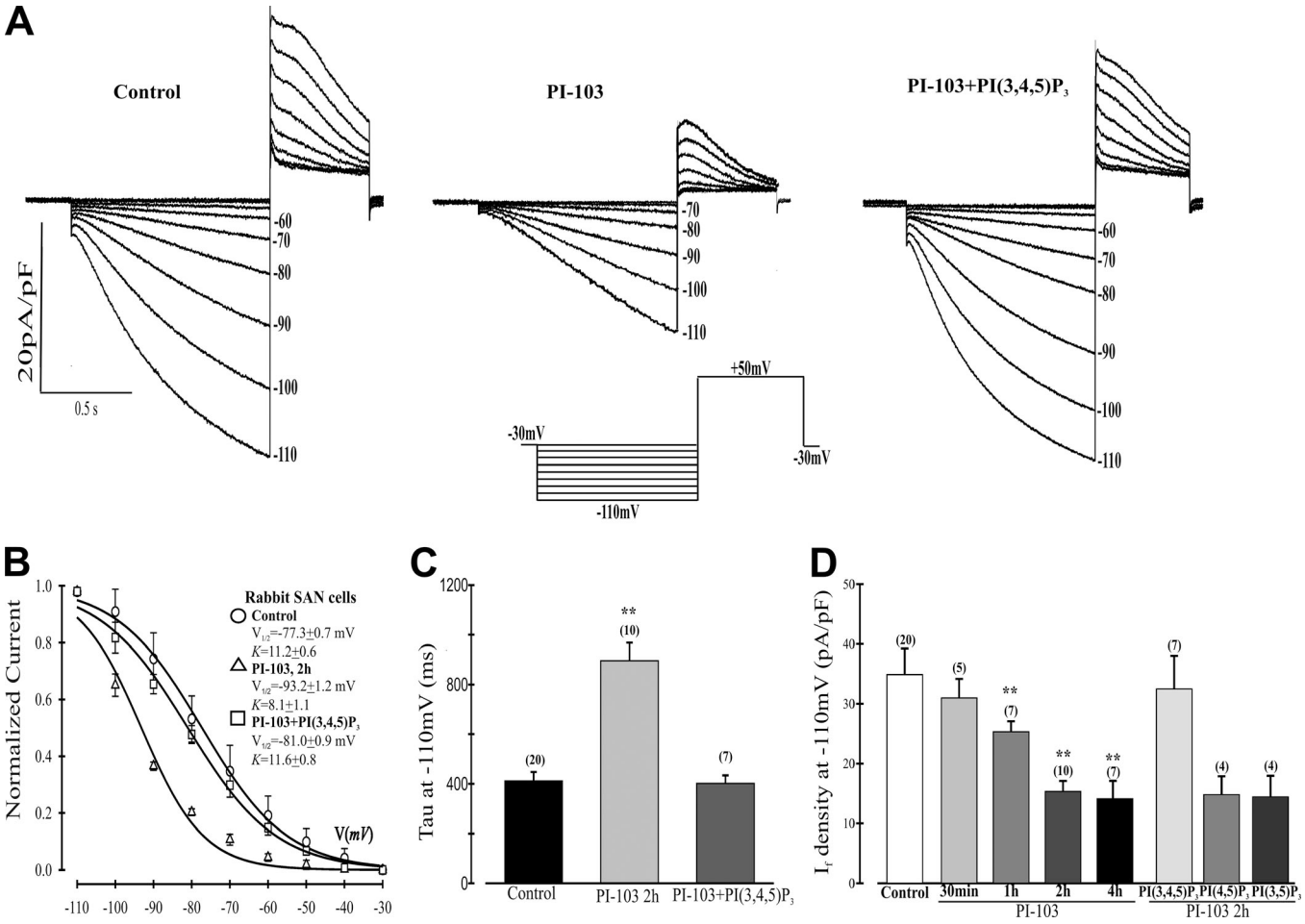

Figure 3. **Effects of PI-103 on I_F in SN cells isolated from rabbit heart. (A)** Representative traces of I_F activation. Cells were untreated (control) or incubated for 2 h with 500 nM PI-103. Some cells treated with PI-103 were then infused with 1 µM PI(3,4,5)P_3 in the pipette solution. Inset: The voltage-clamp protocol for I_F activation was to apply 1-s hyperpolarizing voltage steps ranging from −30 mV to −110 mV in −10 mV increments from a holding potential of −30 mV followed by a depolarizing step to +50 mV for 0.5 s to record the tail currents, after which the preparation was stepped back to the holding potential. **(B)** Boltzmann fit of 1-s IC activation curves for I_F. $V_{1/2}$ and K were derived from the curves. Control, $V_{1/2}$ = −77.3 mV, K = 11.2 mV; PI-103, $V_{1/2}$ = −93.2 mV, K = 8.1 mV; and PI-103 + PI(3,4,5)P_3, $V_{1/2}$ = −81.0 mV, K = 11.6 mV. **(C)** Mean time constants (τ) from a single exponential fit of I_F measured at −110 mV. **, P < 0.01 versus control. **(D)** Summary data of I_F density measured at −110 mV from a holding potential of −30 mV. Cells were incubated with PI-103 for the times indicated before patching with or without infusion of 1 µM PI(3,4,5)P_3 or the control lipids phosphatidylinositol 4,5-bisphosphate (PI(4,5)P_2) or phosphatidylinositol 3,5-bisphosphate (PI(3,5)P_2). **, P < 0.05 versus control. Numbers above the bars indicate the number of cells examined in C and D. *n* values for C also apply to B. Summarized data show mean ± SEM.

shifts in the time constant of activation (τ). τ at −110 mV was more than doubled in PI-103–treated cells, and this alteration was completely reversed by PI(3,4,5)P_3 (Fig. 3 C).

Because the 1-s pulses employed yield currents that are far from SS at some voltages, we used the well-known exponential decay of I_F to generate theoretical SS activation curves for each of the voltage clamp conditions in this experiment. Fig. S1 shows that the fit to SS is indistinguishable from experimentally generated current traces for the first second. Fig. S2 shows the SS fits for activation curves under the control, PI-103, and PI-103 + PI(3,4,5)P_3 conditions. The midpoints of activation were −72.8 mV, −87.9 mV, and −76.8 mV, respectively. Thus, each of the SS activation curves has a more positive activation than its IC counterpart. However, the differences between the experimental conditions are minimal. For control versus PI-103, the negative shifts were 15.9 mV or 15.1 mV for IC or SS, respectively. For PI-103 versus PI-103 + PI(3,4,5)P_3, there were positive shifts of 12.2 mV or 11.1 mV for IC or SS, respectively.

Finally, we quantified the time dependence of PI-103–induced inhibition of I_F by incubating SN myocytes for increasing times with the inhibitor and calculating current density at −110 mV. There was a progressive decrease in IC I_F current density starting at 30 min. This became significant at 1 h and reached an almost maximal level by 2 h (Fig. 3 D). In cells exposed to PI-103 for 2 h, infusion of PI(3,4,5)P_3 through the patch pipette caused the IC current density to return to near control levels (Fig. 3 D). However, substitution of either of two control phospholipids, phosphatidylinositol 4,5-bisphosphate (PI(4,5)P_2) or phosphatidylinositol 3,5-bisphosphate (PI(3,5)P_2), for PI(3,4,5)P_3 in the pipette solution had no effect on the PI-103–induced reduction in I_F current density at −110 mV in IC conditions, further indicating a specific role for PI3K inhibition.

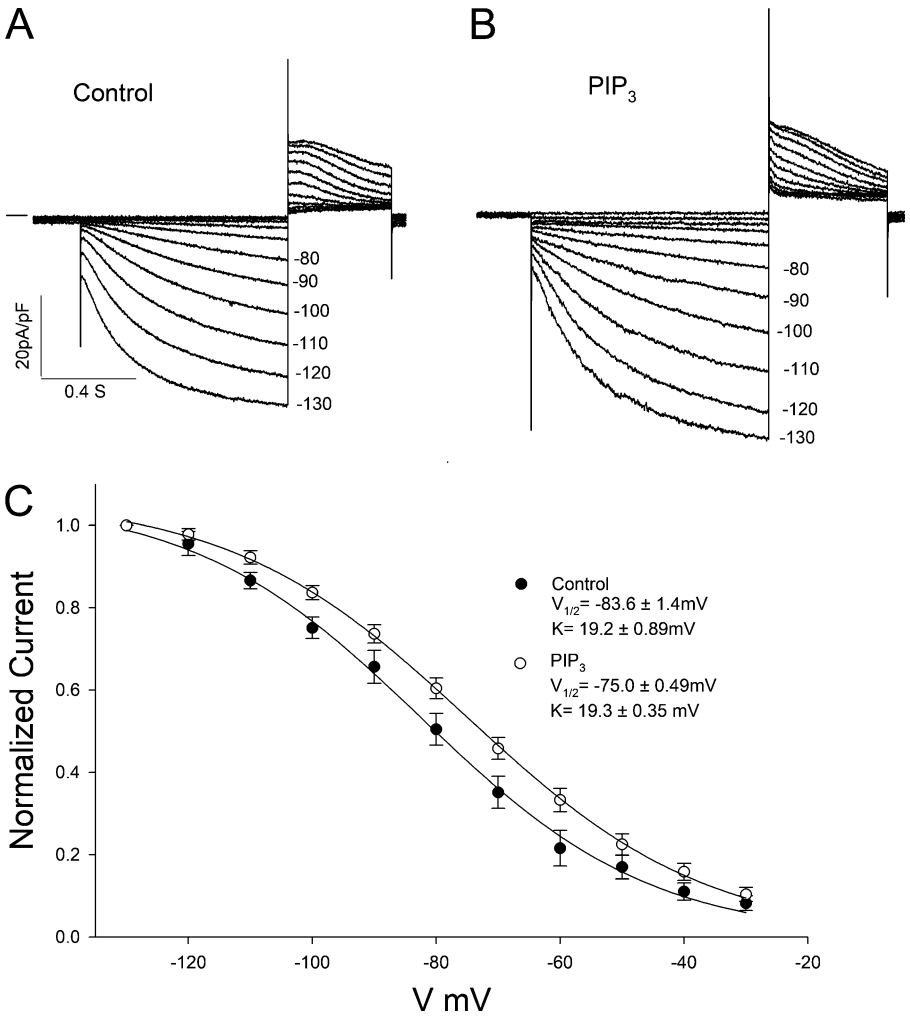

Figure 4. **Effects of PI(3,4,5)P_3 on I_F in SN cells isolated from rabbit heart. (A and B)** Traces of I_F activation in (A) control cells and (B) cells infused with 1 µM PI(3,4,5)P_3 in the patch pipette. **(C)** Boltzmann fit of IC activation curves for I_F. Control (n = 10), $V_{1/2}$ = −83.6 mV, K = 19.2 ± 0.89 mV; PI(3,4,5)P_3 (n = 25), $V_{1/2}$ = −73.7 mV, K = 19.3 ± 0.35 mV. Summarized data show mean ± SEM.

Current densities in Table S1 calculated from SS activation (see Materials and methods) show that PI-103 in the absence or presence of PI(3,4,5)P_3 caused no significant change in I_F magnitude at −110 mV, where the current is almost fully activated.

We next asked whether the control I_F activation curve reflects a maximal effect due to PI3K signaling. To answer this question, we added PI(3,4,5)P_3 to the pipette solution. The results in Fig. 4, A and B, show the raw data in control conditions and with addition of PI(3,4,5)P_3, respectively. Fig. 4 C shows the IC activation curves, which had midpoints of −83.6 mV (control) and −75.0 mV (PI(3,4,5)P_3). Thus, the dynamic range of responsiveness to PI3K signaling is 24.5 mV (which is equal to the sum of the differences of the $V_{1/2}$s of PI-103 and PI(3,4,5)P_3 from the control values) in IC conditions. Midpoints calculated from the theoretical SS curves in Fig. S3 were more positive than those calculated from the IC data (−73.7 mV [control] and −63.1 mV [PI(3,4,5)P_3]). Again, the difference between the shifts in IC and SS activation curves was small (PI(3,4,5)P_3 caused a positive shift of 8.6 mV or 10.6 mV for IC or SS, respectively), and I_F density at −110 mV was not significantly different in the two conditions at SS (Table S1).

Although the SN rhythm is myogenic in origin, the autonomic nervous system modulates both I_F and sinus rate (DiFrancesco, 2006). Since sympathetic and parasympathetic stimulation alter I_F voltage dependence but not amplitude (DiFrancesco, 2006), the results in Fig. 1 (the in situ mouse heart) and Fig. 2 (the in vitro canine SN) suggested that the action of PI-103 is independent of autonomic regulation since although the inputs to the SN remain, there is no feedback control. We therefore investigated whether the shift in voltage dependence of activation we observed with exposure to PI-103 was dependent on the autonomic nervous system. SN myocytes were pretreated for 2 h with PI-103 and then exposed to CCh or Iso before measuring I_F. Fig. 5, A and C, shows that the IC I_F current density at −110 mV was further reduced upon exposure to CCh and increased in cells exposed to Iso. These differences in amplitude and current density are consistent with the difference in kinetics and open probability induced by the autonomic agonists. The IC activation curves in Fig. 5 B demonstrate a 6.9-mV negative shift in $V_{1/2}$ induced by CCh ($V_{1/2}$ = −90.2 ± 1.2 mV [PI-103] versus −97.1 ± 1.9 mV [PI-103 + CCh]), while Iso induced an 11.8-mV positive shift in IC midpoint voltage ($V_{1/2}$ = −78.4 ± 1.3 mV [PI-103 + Iso]). The dynamic range of autonomic responsiveness in the presence of PI-103 is 18.7 mV ([$V_{1/2}$ + Iso] − [$V_{1/2}$ + CCh]) in IC conditions. This is very close to the value of 19.5 mV in control conditions reported by Zaza et al. (1996). We fit the data for the PI-103 and PI-103 + Iso conditions to SS and calculated midpoint voltages of −87.9 mV and −74.3 mV,

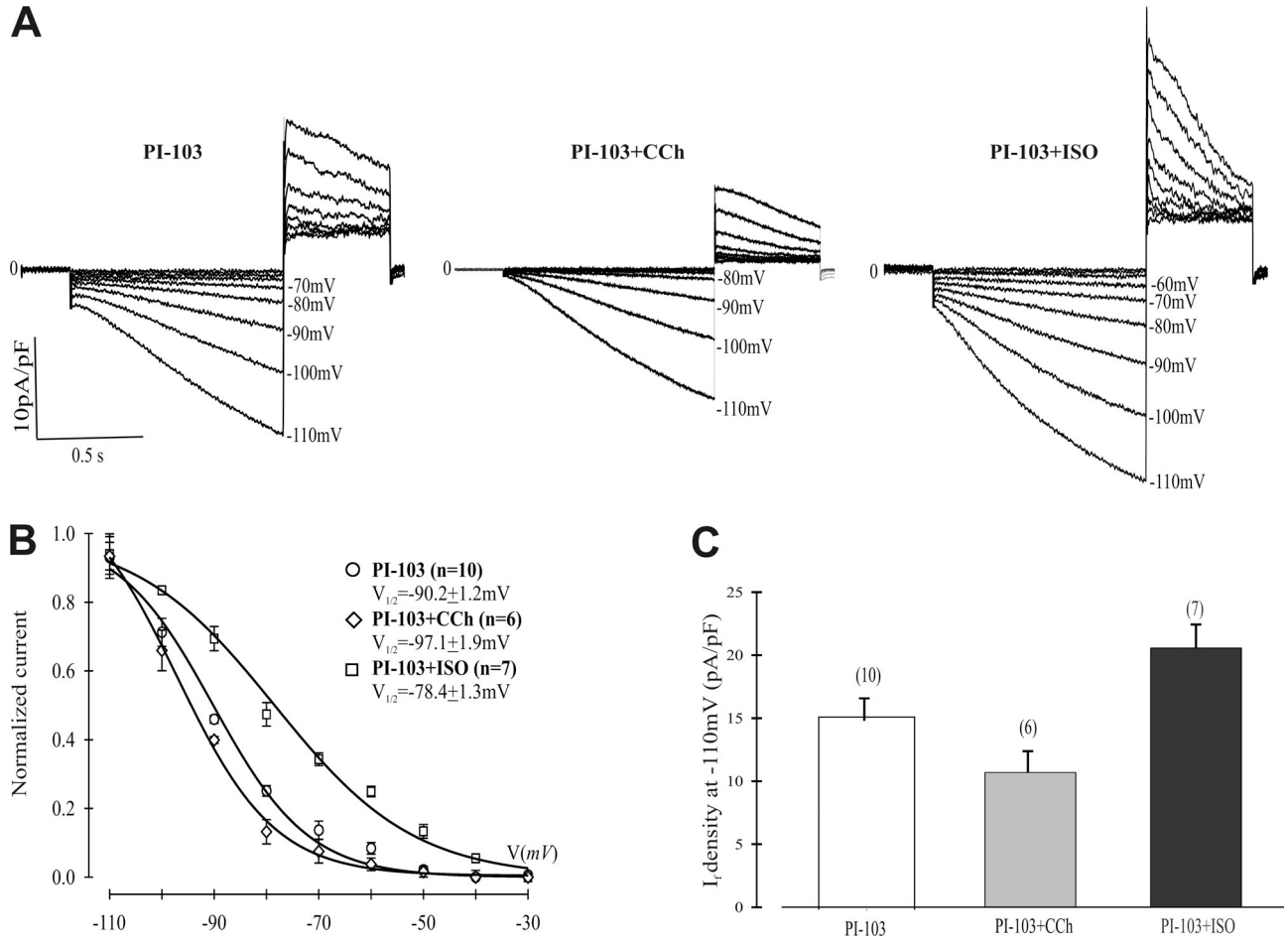

Figure 5. **Effects of CCh or Iso on I_F in isolated rabbit SN cells pretreated with PI-103. (A)** Typical traces of I_F activation in cells treated for 2 h with 500 nM PI-103 alone or treated with PI-103 and then exposed to 1 µM CCh or 10 µM Iso for 5 min. **(B)** Boltzmann fit of 1-s IC activation curves for I_F. $V_{1/2}$ and K were derived from the curves. PI-103, $V_{1/2}$ = −90.2 mV, K = 9.2 mV; PI-103 + CCh, $V_{1/2}$ = −97.1 mV, K = 9.3 mV; PI-103 + Iso, $V_{1/2}$ = −78.4 mV, K = 13.4 mV. **(C)** Summary data of I_F density measured at −110 mV from a holding potential of −30 mV. Numbers above the bars indicate the number of cells examined. Summarized data show mean ± SEM.

respectively (Fig. S4), yielding shifts of 11.8 mV (IC) or 13.6 mV (SS). There was no significant difference in the SS I_F current density at −110 mV between PI-103 + Iso and other conditions (Table S1).

Discussion

We initiated our investigation because of the wide range of ion currents we found to be altered by inhibition of PI3K and because of the relevance of these channel effects to both drug action and manifestations of type 2 diabetes (Lu et al., 2012, 2013). We found that in the absence of regulation via normal feedback autonomic stimulation, PI3K inhibition reduced heart rate in the perfused mouse heart, and the β agonist Iso increased heart rate under these conditions. To confirm these observations in a larger adult animal frequently used as a human surrogate in electrophysiologic studies, we studied the effect of PI3K inhibition on SN isolated from the canine heart to eliminate feedback autonomic regulation. The PI3K inhibitor PI-103 again lowered spontaneous beating rate, and addition of Iso increased rate in a reversible manner. These two results suggested that PI3K inhibition of SN rate might be independent of autonomic regulation.

To further investigate the origins of this change in spontaneous rate, we investigated the properties of the pacemaker current I_F by patch clamp in rabbit SN myocytes in which there are no autonomic nerve endings. Addition of the nonspecific PI3K blocker had a time-dependent effect, which was first observed at 30 min. The amplitude of the current declined over 2 h of treatment, and the midpoint of the voltage dependence of activation shifted to more negative potentials (−15.9 mV) in IC conditions. We also performed experiments adding $PI(3,4,5)P_3$ to the pipette solution. This induced an 8.6-mV positive shift in IC conditions with no change in SS tail maximal current amplitude. Thus, our observations on I_F were entirely consistent with the observed changes in SN rate. In addition, our studies of the canine SN action potential indicated a PI-103–induced negative shift in MDP and a decrease in EDD. These changes are also consistent with the observed actions on I_F, since our SS calculations (Table S1) suggested there was no change in maximal I_F tail current density at −110 mV, where the SS activation curves

are virtually fully activated. Our studies of spontaneous activity in the intact mouse heart and the isolated canine SN suggested that autonomic regulation was unaltered by PI3K inhibition. Since autonomic regulation is evidenced by a shift in the midpoint of the voltage dependence of activation, we examined the effects of both muscarinic stimulation and sympathetic stimulation on the $V_{1/2}$ of I_F. CCh caused a negative shift while Iso caused a positive shift in the midpoint of activation in IC conditions. The dynamic range (midpoint Iso–midpoint CCh) of 18.7 mV was entirely consistent with the previously reported value of 19.5 mV in control conditions (Zaza et al., 1996). SS calculations suggest there was no change in SS I_F tail current density at −110 mV in the presence of Iso.

The novel action of PI3K inhibition on pacemaker activity is important for several reasons. First, inhibition of PI3K is a mechanism by which some drugs cause long QT syndrome (Lu et al., 2012; Yang et al., 2014). Second, reduced activity of cardiac PI3K is an expected outcome in type 2 diabetes. It is interesting to note that while basal heart rate is increased in diabetic people (Ewing et al., 1981; Hume et al., 1986), exposure to PI-103 caused rate slowing in the ex vivo mouse heart and the isolated canine SN where no sympathetic feedback is available. Presumably, this difference results from the well-known increase in sympathetic and decrease in parasympathetic tone that accompany diabetes. Our results raise the possibility that a myogenic reduction in heart rate caused by PI3K inhibition could be a factor mediating these changes in sympathetic and parasympathetic tone in type 2 diabetes. Importantly, a novel pathway has been defined that regulates heart rate independently of the autonomic nervous system. This presents a target for novel drug development aimed at normalizing heart rate in diabetes and other conditions of tachycardia or bradycardia.

Acknowledgments

This project was funded in part by the National Institutes of Health (DK108989 to R.Z. Lin and HL126774 to I.S. Cohen), and the U.S. Department of Veterans Affairs Merit Review (BX004083 to R.Z. Lin).

The authors declare no competing financial interests.

Author contributions: R.Z. Lin conceived of the first experiment, analyzed the data, and cowrote the manuscript. Z. Lu designed, performed, and analyzed the patch-clamp data in Fig. 3 and Fig. 5. E.P. Anyukhovsky executed and analyzed the experimental data for Fig. 2. Y.P. Jiang executed the experiment in Fig. 1 and helped analyze the data. H.Z. Wang designed and analyzed the experiment in Fig. 4. J. Gao helped analyze the data in the supplemental figures and Table S1. M.R. Rosen helped design the studies and analyze the data in Fig. 2. L.M. Ballou helped analyze all the data and cowrote the manuscript. I.S. Cohen oversaw the execution of the patch-clamp experimental design and analysis, and cowrote the manuscript.

Eduardo Ríos served as editor.

Submitted: 19 November 2018
Revised: 1 May 2019
Accepted: 3 June 2019

References

DiFrancesco, D. 2006. Funny channels in the control of cardiac rhythm and mode of action of selective blockers. *Pharmacol. Res.* 53:399–406. https://doi.org/10.1016/j.phrs.2006.03.006

DiFrancesco, D., A. Ferroni, M. Mazzanti, and C. Tromba. 1986. Properties of the hyperpolarizing-activated current (if) in cells isolated from the rabbit sino-atrial node. *J. Physiol.* 377:61–88. https://doi.org/10.1113/jphysiol.1986.sp016177

Eisner, D.A., and E. Cerbai. 2009. Beating to time: calcium clocks, voltage clocks, and cardiac pacemaker activity. *Am. J. Physiol. Heart Circ. Physiol.* 296:H561–H562. https://doi.org/10.1152/ajpheart.00056.2009

Ewing, D.J., I.W. Campbell, and B.F. Clarke. 1981. Heart rate changes in diabetes mellitus. *Lancet.* 1:183–186. https://doi.org/10.1016/S0140-6736(81)90061-1

Hume, L., G.D. Oakley, A.J. Boulton, C. Hardisty, and J.D. Ward. 1986. Asymptomatic myocardial ischemia in diabetes and its relationship to diabetic neuropathy: an exercise electrocardiography study in middle-aged diabetic men. *Diabetes Care.* 9:384–388. https://doi.org/10.2337/diacare.9.4.384

Lu, Z., C.Y. Wu, Y.P. Jiang, L.M. Ballou, C. Clausen, I.S. Cohen, and R.Z. Lin. 2012. Suppression of phosphoinositide 3-kinase signaling and alteration of multiple ion currents in drug-induced long QT syndrome. *Sci. Transl. Med.* 4:131ra50. https://doi.org/10.1126/scitranslmed.3003623

Lu, Z., Y.P. Jiang, C.Y. Wu, L.M. Ballou, S. Liu, E.S. Carpenter, M.R. Rosen, I.S. Cohen, and R.Z. Lin. 2013. Increased persistent sodium current due to decreased PI3K signaling contributes to QT prolongation in the diabetic heart. *Diabetes.* 62:4257–4265. https://doi.org/10.2337/db13-0420

Sosunov, E.A., and E.P. Anyukhovsky. 2012. Differential effects of ivabradine and ryanodine on pacemaker activity in canine sinus node and purkinje fibers. *J. Cardiovasc. Electrophysiol.* 23:650–655. https://doi.org/10.1111/j.1540-8167.2011.02285.x

Tromba, C., and I.S. Cohen. 1990. A novel action of isoproterenol to inactivate a cardiac K+ current is not blocked by beta and alpha adrenergic blockers. *Biophys. J.* 58:791–795. https://doi.org/10.1016/S0006-3495(90)82422-X

Yang, T., Y.W. Chun, D.M. Stroud, J.D. Mosley, B.C. Knollmann, C. Hong, and D.M. Roden. 2014. Screening for acute IKr block is insufficient to detect torsades de pointes liability: role of late sodium current. *Circulation.* 130:224–234. https://doi.org/10.1161/CIRCULATIONAHA.113.007765

Zaza, A., R.B. Robinson, and D. DiFrancesco. 1996. Basal responses of the L-type Ca2+ and hyperpolarization-activated currents to autonomic agonists in the rabbit sino-atrial node. *J. Physiol.* 491:347–355. https://doi.org/10.1113/jphysiol.1996.sp021220